# Modeling the Early Stages of Thin Film Formation by Energetic Atom Deposition

C.A. STONE and N.M. GHONIEM

The early stages of thin film formation are described by a simple hybrid model that couples a set of discrete kinetic rate equations to a Fokker-Planck (FP)-type continuum. Unique features of the atomic processes in energetic particle deposition are outlined and discussed. A thermal atom deposition process is benchmarked with Zinsmeister's analytical theory[17] to demonstrate the simplicity and accuracy of the model. This simplicity allows extensions to the treatment of energetic particle effects and the growth of multilayers of atoms. It is shown that the model explains the major features of the early stages of atomic clustering.

## I. INTRODUCTION

THE advent of energetic atom deposition technologies has resulted in new production techniques for synthesizing thin films and coatings. Energetic neutral atoms and charged particles impinge on a surface with energies far in excess of the thermal energy of an average lattice atom. The simultaneous action of a number of unique atomic processes (sputtering, implantation, nucleation, heating, and migration) produces films which possess promising properties. As such, thin film formation by energetic particles is fundamentally different from atomic deposition processes involving thermal particles (*e.g.*, evaporation and condensation).

A number of energetic atom deposition processes are currently being used for surface modification and thin film production purposes. These processes use a high vacuum system to condense superthermal free particles on a host material. Ion-beam deposition systems deposit ionized material directly onto a surface. Similar to ion-beam deposition is ionized cluster-beam deposition, in which a cluster of atoms is ionized and accelerated toward a substrate. Upon impact on the substrate, the cluster dissolves into individual atoms. In ion-beam sputtering deposition (IBSD), an ion beam is used to sputter a solid target; these sputtered target atoms then modify the surface to be processed. Reactive ion-beam sputtering deposition is similar in principle to IBSD, but reactive molecules are introduced during the deposition process, either in the ion beam or in the gaseous phase. Dual-beam sputtering deposition is also similar to IBSD; however, an additional ion beam is used to directly bombard the growing film. An excellent review of these ion-beam processes and their applications can be found in Reference 1.

Other energetic atom deposition methods which use plasmas include radio frequency (RF) bias sputtering, magnetron sputtering, triode sputtering, ion plating, activated reactive evaporation, and plasma-enhanced chemical vapor deposition.[2] These plasma processing technologies have significantly enhanced the semiconductor fabrication industry.[3] Additionally, investigations of the surface modification of materials by plasma bombardment have been performed in order to develop plasma-interactive components for fusion reactor systems.[4,5,6]

The high energies of the bombarding particles actually damage a surface by creating near-surface defects and partially destroying a growing film. However, numerous benefits of energetic atom deposition processes manifest themselves in the final surface characteristics of the thin films produced. The surface mobility of energetic atoms is higher than corresponding thermal deposition techniques; thus, epitaxial films can be produced at lower substrate temperatures. Superior coating adhesion is also achieved because of ion-beam mixing at the film-substrate interface. From an industrial point of view,[7] such processes alter the mechanical, chemical, electrical, optical, and tribological properties of a surface. The surfaces created can have high wear and corrosion resistance, reduced friction, improved fatigue performance, good adhesive properties, hard diamond-like coatings, and desirable electrical and optical features.

A review of previous atomistic studies, which have tried to assess the nucleation and growth of thin films prepared by thermal deposition methods, is given in Reference 8. Theoretical models of thermal deposition have shown consistency with experimental observations of nucleation and growth. Various assumptions must invariably be made to simplify the computational task and, thus, models of varying degrees of complexity have been proposed. In complicated experimental procedures, thin film synthesis has often been considered a black art;[9] nonetheless, the theoretical attempts at modeling thermal particle deposition have helped in clarifying the relationships between atomistic processes and the macroscopic properties of thin films.

For energetic atom deposition processes, one needs to assess the impact of 1 to 100 eV particles and charged species on a growing film, as well as the impact of energetic clusters. Ion scattering measurement experiments have been developed for the production of well-characterized noble gas and metal ion beams over the energy range of $\leq$20 eV to 10 keV,[10] which should

C.A. STONE, Graduate Student, and N.M. GHONIEM, Professor of Engineering, are with the Mechanical, Aerospace and Nuclear Engineering Department, University of California-Los Angeles, Los Angeles, CA 90024.

This paper is based on a presentation made in the symposium "Irradiation-Enhanced Materials Science and Engineering" presented as part of the ASM INTERNATIONAL 75th Anniversary celebration at the 1988 World Materials Congress in Chicago, IL, September 25–29, 1988, under the auspices of the Nuclear Materials Committee of TMS-AIME and ASM-MSD.

provide insight into particle-surface interactions over energy ranges of interest in energetic atom deposition processes. However, the authors have no knowledge of any comprehensive kinetic theoretical studies on the influence of energetic atom deposition processes on thin film formation.

The purpose of this paper is to develop a comprehensive theoretical model which describes energetic atom deposition processes. Fundamental atomic processes will be identified and described by a set of equations which can be solved to yield information about the resultant thin film formation and structure. Such a study should enable the design of deposition processes to produce desired surface characteristics. Also, fundamental atomistic processes can be identified and related to the macroscopic surface properties.

## II. A MODEL FOR THIN FILM FORMATION

The first step in modeling thin film formation by energetic atom deposition involves identifying the various physical processes which occur when energetic particles impinge on a substrate host. A set of equations can then be developed to describe these processes. In this paper, an atomistic approach is used to model the deposition event, atomic clustering, and thin film formation. To simplify the formulation, we subdivide the problem into five stages: kinetics of the early stages of atomic clustering, energetic atom processes, cluster nucleation and growth, cluster coalescence, and multilayer thin film formation. Each stage is briefly described in this section.

### A. *Kinetics of the Early Stages of Atomic Clustering*

Before describing the early deposition phenomena, a few notational variables will be introduced. As particles are deposited on a substrate to form a thin film, clusters of particles will appear on the substrate, eventually covering the surface and forming a coating. The variable of interest in this study is the cluster density distribution function, $C(x,L,t)$, which is the number of clusters per unit substrate area found on the substrate at time $t$; $x$ is the number of atoms in the cluster, and $L$ is the particular thin film layer on which the cluster is located. The first monolayer of film is defined as $L = 1$; for modeling near-surface substrate layers, $L \leq 0$. The top surface of a growing film structure is denoted by $L_{max}$. The variables $x$ and $y$ will be used to denote the number of atoms in various clusters on the substrate, while $z$ will designate atoms being deposited from a deposition source.

Five processes are identified in the early stages of atomic clustering: energetic atom deposition, direct impingement, cluster evaporation, cluster aggregation, and dissociation. The deposition rate per unit substrate area is given by $q[z,E(z)]$. For single-atom deposition processes, $z = 1$, and $q[1,E(1)]$ represents the single-atom deposition rate, where each particle strikes the substrate with energy $E(1)$. In the case of an ionized cluster-beam deposition process, the depositing species will strike the substrate as clusters of $z$-atom particles, where each cluster of $z$ atoms has an energy $E(z)$. If a deposited cluster completely dissolves after striking the substrate, each particle will transfer an average energy of $\langle E \rangle = E(z)/z$.

Direct impingement occurs when a depositing particle lands directly on an atomic cluster already present on the substrate. Direct impingement effects are usually not important until the later stages of atomic clustering, when a substantial portion of the substrate surface is covered with growing clusters. Nonetheless, the rate per unit substrate area at which an $x$-atom cluster grows by direct impingement is given by $q[z,E(z)]\sigma_z(x)C(x,L,t)$, where $\sigma_z(x)$ is the probability (in units of area) that a $z$-particle cluster from the deposition process will directly impinge on an $x$-atom cluster. The value of $\sigma_z(x)$ depends on both the size and geometry of the clusters present on the substrate.

It should be obvious that the net effect of the deposition process is to place atoms on the substrate. Once on the substrate, these atoms can migrate and participate in a variety of events. If an atom has enough thermal energy, it may evaporate off the substrate. Single atoms are more likely to evaporate than actual clusters. For consistency, the evaporation rate for an $x$-atom surface cluster ($L = L_{max}$) will be defined as $C(x,L_{max},t)/\tau_{evap}(x,L_{max})$, where $\tau_{evap}(x,L_{max})$ is a characteristic time that an $x$-atom cluster remains on the surface before evaporating. The value of $\tau_{evap}(x,L_{max})$ depends on the substrate temperature and on the binding energies of cluster atoms.

During the early stages of atomic clustering, two clusters migrating across the substrate surface may aggregate into a larger cluster. The rate at which $x$- and $y$-atom clusters aggregate together [forming an $(x + y)$-atom cluster] is given by $w_y(x)C(x,L,t)C(y,L,t)$, and aggregation is assumed to occur in the same atomic layer. The aggregation rate constant, $w_y(x)$, is the rate (area/time) at which $x$- and $y$-atom clusters aggregate and depends on the cluster sizes as well as the substrate temperature and lattice constant.

Because of dissociation processes, large clusters may break up into smaller ones. The rate at which an $x$-atom cluster dissociates from a $y$-atom cluster (for $x < y$) is given by $\alpha_y(x)C(y,L,t)$, where $\alpha_y(x)$ is the dissociation frequency of an $x$-atom cluster from a $y$-atom cluster. The term $\alpha_y(x)$ becomes an increasingly complex function, if one tries to account for all of the possible dissociation paths that a large $y$-atom cluster can undergo; however, the energetics of dissociation allow for simplifications.

### B. *Energetic Atom Processes*

When an energetic atom strikes a surface, a variety of synergistic effects can occur. Surface defects are produced, atomic mixing occurs, and energy is dissipated in the form of local surface heating. With this in mind, four energetic atom deposition effects are identified which will play a major role in the creation and destruction of a growing thin film. These effects include particle reflection, surface sputtering, implantation, and cluster resolution.

Not all of the energetic particles that strike a substrate actually stick. The particle reflection coefficient for the depositing species will be defined as $R_f[E(z),\Theta(L)]$, where

$\Theta(L)$ is the angle of incidence of the depositing species with respect to layer $L$. The fraction of incident particles which actually make it to the substrate is then $\{1 - R_f[E(z), \Theta(L)]\}$; consequently, the effective deposition rate on the substrate is $\{1 - R_f[E(z), \Theta(L)]\}q[z, E(z)]$.

Particles that do not reflect off the substrate may thermally settle on the substrate surface. Depending on the particle energy, however, sputtering or implantation may result. Sputtering erodes the top surface layers, whereas the implantation mechanism drives the impinging species into the near-surface layers. To assess the effects of sputtering, the sputtering yield, $S[E(z), \Theta(L)]$, will be defined as the number of atoms in layer $L$ that are sputtered out of the film (or the substrate, if $L \leq 0$) per incident of deposited species of energy $E(z)$. Implantation can similarly be characterized by defining an implantation parameter $I[E(z), L]$, which designates which fraction of the deposited species of energy $E(z)$ implants itself in layer $L$.

Probably the most difficult effect to assess readily is the cluster resolution rate. Although similar to direct impingement, which involves the incorporation of the depositing species on a growing cluster, the cluster resolution process occurs when the depositing species has enough energy to break up a growing cluster if it impinges directly on it. At the present time, it is not known exactly how much energy is required to break up a growing cluster or how the cluster will physically split. Obviously, the larger the cluster, the more energy is required to completely dissolve it into individual atoms. Nonetheless, the probability of a 10-atom cluster breaking up into ten individual atoms or two 5-atom clusters is unknown. Molecular dynamics simulations may shed some light on this process. In this work, the cluster resolution parameter, $R_s[x, L, E(z)]$, will be defined as the probability of an $x$-atom cluster located in layer $L$ to break up into individual atoms when struck by the depositing species of energy $E(z)$.

### C. *Nucleation and Growth*

The net result of the deposition process and the atomistic effects described in Sections II-A and B is to produce atoms on a substrate that can nucleate into a size distribution of small clusters. These clusters may grow as two- or three-dimensional entities, forming various geometrical patterns (*e.g.*, islands, spheres, needles, cones, *etc.*). During the early stages of the deposition process, when less than 10 pct of the substrate surface is covered, direct impingement and cluster resolution effects are negligible because of the small substrate coverage. Although these factors will become more prominent as the deposition process proceeds, of more concern is the influence of cluster coalescence and mobility.

### D. *Cluster Coalescence*

It has been known that cluster mobility decreases with increasing cluster size; hence, only small clusters are mobile. From this standpoint, small clusters will be the active species in the aggregation process, and the aggregation rate constant, $w_y(x)$, will assume significant values only for small size clusters. Nonetheless, as more and more of the substrate is covered, clusters will not have to move over the substrate to aggregate into larger clusters. Instead, the substrate will be so crowded that the clusters will simply impinge on each other, coalescing into larger size ones.

When coalescence is included in the deposition process, the clustering problem clearly becomes more complicated. In this case, one must consider clusters of size $x$ interacting with all other clusters of size $y$. Since coalescence does not play a significant role until the later stages of the film formation process, when $x$ and $y$ are large, one has a broad distribution of cluster sizes to consider. Here, one must conserve the total number of atoms present on the substrate at all times during coalescence events. This involves adding additional source terms to a conservation equation that we derive in Section III (for details, see Appendix A).

### E. *Multilayer Thin Film Formation*

The nucleation and coalescence phenomena eventually result in the formation of a thin film on the substrate. As the deposition process proceeds, however, multiple layers of clusters will form simultaneously. Multilayer thin film formation proceeds because of the two- and three-dimensional nature of the growing clusters, stacking effects as direct impingement occurs, sputtering, resolution phenomena, *etc.* In other words, one complete monolayer will not form before another monolayer grows on top. Different layers of the film will grow concurrently.

The cluster density distribution function, $C(x, L, t)$, has previously only been related to a particular thin film layer, $L$. As thin film formation occurs, the various film layers will influence one another through interlayer aggregation, coalescence, implantation effects, sputtering, *etc.* Consequently, we must keep an inventory of such interlayer effects. In so doing, we should be able to accurately reconstruct $C(x, L, t)$ and determine the resulting thin film structure and morphology.

## III. APPLICATION OF THE MODEL TO THERMAL ATOM DEPOSITION

The atomic clustering model outlined in Section II includes many processes that occur during thin film formation by energetic atom deposition. In several theoretical studies of thin films, a kinetic formulation of hierarchical discrete rate equations has been used to describe cluster sizes.[11–18] These rate equations are coupled, nonlinear, and extremely complex. Thus, they are difficult to solve unless some simplifying physical assumptions are introduced. From a computational standpoint, one must deal with a large system of equations to obtain specific clustering details (*e.g.*, if the largest cluster contains 100 atoms, then 100 simultaneous equations must be solved for each layer of the film considered).

In our approach, we retain the relevant clustering physics by solving a system of discrete kinetic rate equations that are coupled to a continuum FP-type equation. In this manner, the number of equations which must be solved is not dictated by the largest cluster size in our system.

The ideas presented here for the comprehensive kinetic model must be checked by systematic and detailed

computations to determine the influence of each process on the characteristics of the evolving thin film. This task can be best accomplished by model correlations with experimental data. As a first step toward this goal, in this section, we present a simplified version of the model that is applicable for the early stages of thin film formation from thermally deposited atoms. This will allow a validation of our model against existing theories which have already been correlated to experimental data. It will also be demonstrated that a relatively less intensive computational model, using only a small number of equations, can yield information on all relevant aspects of atomic clustering.

Various simplifications immediately arise when one considers only thermal particle deposition, since all of the energetic atom processes are neglected. Such particles may also be considered monoenergetic. In order to benchmark our results with Zinsmeister's theory,[17] the following additional assumptions must be invoked:

(1) Thermal single atoms are deposited at a rate of $q$ atoms/cm$^2$/s.
(2) Cluster growth and decay result only from mobile single atoms.
(3) Only single atoms can evaporate off the substrate.
(4) Aggregation and dissociation rate constants are size independent.
(5) The model represents the early stages of deposition (*i.e.*, substrate coverage ≤10 pct) for the first atomic monolayer.

Assumption 1 implies that $q[z, E(z)] = q$. Assumption 2 implies that $w_y(x) = w_1(x)$ and $\alpha_y(x) = \alpha_1(x)$. Assumption 3 implies that $\tau_{evap}(x, L) = \tau_{evap}(1, 1) = \tau_{evap1}$ (the average time a single atom stays on the substrate before evaporating). Assumption 4 implies that $w_1(x) = w$ and $\alpha_1(x) = \alpha$. And, finally, assumption 5 implies that $C(x, L, t) = C(x, 1, t) = C(x, t)$ (the density of $x$-atom clusters on the substrate). Before attempting to solve for the comprehensive model, it is important first to establish the features of the model by comparing it with Zinsmeister's simplified theory of atomic clustering.[17,18]

Applying these assumptions to our model allows us to write a series of discrete kinetic rate equations for clusters containing up to $X_{max}$ atoms:

$$\frac{\partial C(1,t)}{\partial t} = q + \alpha\left[\sum_{y\geq 2}^{X_{max}} C(y,t)(\delta_{y2}+1)\right] - \frac{C(1,t)}{\tau_{evap1}} - wC(1,t)\left[\sum_{x\geq 1}^{X_{max}} C(x,t)\right] \quad [1]$$

$$\frac{\partial C(x,t)}{\partial t} = \left(1-\frac{\delta_{x2}}{2}\right) wC(1,t)C(x-1,t) + \alpha C(x+1,t) - wC(1,t)C(x,t) - \alpha C(x,t) \qquad \text{for } 2 \leq x \leq X_{max} \quad [2]$$

where $\delta_{ab} = 1$, if $a = b$, and $\delta_{ab} = 0$, if $a \neq b$. The successive terms on the right-hand side of Eq. [1] represent the deposition rate of single atoms on the substrate, the production of single atoms due to the dissociation of larger clusters, the evaporation of single atoms off the substrate, and the aggregation of single atoms with larger clusters. Equation [2] states that the density of all other size clusters increases by the aggregation of a single atom with an $(x-1)$-atom cluster and the dissociation of an $(x+1)$-atom cluster and decreases when a single atom aggregates with an $x$-atom cluster or an $x$-atom cluster dissociates.

To avoid writing $X_{max}$ discrete equations, a continuum equation is derived for $3 \leq x \leq X_{max}$. To obtain such a continuum equation, we expand the cluster densities $C(x-1,t)$, $C(x,t)$, and $C(x+1,t)$ in Eq. [2] in a second-order Taylor series about $x$. This procedure yields the following continuum equation for $3 \leq x \leq X_{max}$:

$$\frac{\partial C(x,t)}{\partial t} \simeq -\frac{\partial J(x,t)}{\partial x} \quad [3]$$

where the nucleation current $J(x,t)$ is defined as

$$J(x,t) = F(t)C(x,t) - \frac{\partial}{\partial x}[D(t)C(x,t)] \quad [4]$$

and the drift and dispersion coefficients, $F(t)$ and $D(t)$, as

$$F(t) = wC(1,t) - \alpha \quad [5]$$

$$D(t) = \frac{1}{2}[wC(1,t) + \alpha] \quad [6]$$

Equation [3] is of the FP-type, consisting of systematic drift and random dispersion terms. Studies of swelling and irradiation creep[19] have used this same technique to model the nucleation of voids and dislocation loops in irradiated microstructures.

It should be noted that the continuum equation (Eq. [3]) and the general discrete kinetic equation (Eq. [2]) are both valid for $3 \leq x \leq X_{max}$. In order to couple the discrete equations to the continuum, a transition cluster size, $X_c$, will be defined as the smallest cluster size described by the continuum equation. Thus, atomic clustering is described by a set of discrete kinetic equations for $1 \leq x \leq (X_c - 1)$ and by a continuum equation for $X_c \leq x \leq X_{max}$. We now proceed by taking the zero, first, and second moments of Eq. [3] to obtain our complete system of simplified clustering equations, described below:

$$\frac{\partial C(1,t)}{\partial t} = q - \frac{C(1,t)}{\tau_{evap1}} - wC^2(1,t) + \alpha C(2,t) - F(t)\left[\sum_{x\geq 2}^{X_c-1} C(x,t)\right] - F(t)C_{tot} \quad [7]$$

$$\frac{\partial C(2,t)}{\partial t} = \frac{1}{2}wC^2(1,t) - 2D(t)C(2,t) + \alpha C(3,t) \quad [8]$$

$$\frac{\partial C(x,t)}{\partial t} = wC(1,t)C(x-1,t) - 2D(t)C(x,t) + \alpha C(x+1,t) \qquad \text{for } 3 \leq x \leq (X_c - 1) \quad [9]$$

$$\frac{\partial C_{tot}}{\partial t} = J(X_c,t) \quad [10]$$

$$\frac{\partial\langle x\rangle}{\partial t} = \frac{[(X_c - \langle x\rangle)J(X_c,t) + D(t)C(X_c,t)]}{C_{tot}} + F(t) \quad [11]$$

$$\frac{\partial M_2}{\partial t} = \frac{[(X_c - \langle x\rangle)^2 - M_2]J(X_c,t)}{C_{tot}} + 2D(t)\left[\frac{(X_c - \langle x\rangle)C(X_c,t)}{C_{tot}} + 1\right] \quad [12]$$

where $C_{tot}$ is the total continuum cluster density, $\langle x\rangle$ is the average size of the continuum clusters, and $M_2$ is the second central moment (*i.e.*, the variance) of the continuum cluster distribution function. The continuum cluster density at $X_c$ must be obtained by reconstructing the distribution function from its moments. A convenient procedure is to assume that the continuum cluster distribution function is Gaussian, allowing us to approximate $C(X_c, t)$ as

$$C(X_c,t) = \frac{C_{tot}}{\sqrt{2\pi M_2}} \exp\left[-\frac{(X_c - \langle x\rangle)^2}{2M_2}\right] \quad [13]$$

and the nucleation current going into the continuum, $J(X_c, t)$, as

$$J(X_c,t) = wC(1,t)C(X_c - 1,t) - \alpha C(X_c,t) \quad [14]$$

Equations [7] through [12] represent a hybrid method of solving the clustering equations, since a set of discrete kinetic equations is self-consistently coupled to a continuum. These equations are nondimensionalized (see Appendix B) and then numerically integrated for the relevant clustering parameters.

## IV. SOLUTIONS AND COMPARISON WITH PREVIOUS WORK

The complete system of dimensionless simplified clustering equations (see Appendix B for details) was solved for a thermal atom deposition case previously studied by Zinsmeister.[17] In particular, we investigated his results for $q = 10^{15}$ atoms/cm$^2$/s, $\tau_{evap1} = 10^{-7}$ s, $w = 2 \times 10^{-3}$ cm$^2$/s, and $\alpha = 0$. For our study, this means $\beta = 0.02$ and $\gamma = 0$. Before the deposition process begins, there are no clusters present on the substrate. Consequently, and for computational convenience, we initially set all cluster densities equal to 0, $C_{tot} = \varepsilon$, $\langle x\rangle = X_c$, and $M_2 = \varepsilon$, where $\varepsilon = 1 \times 10^{-20}$. The number of atoms in the smallest cluster described by our continuum equation, $X_c$, was selected to be 5 (other choices of $X_c$ were found not to alter the results). Thus, we only have seven equations which must be solved to describe atomic clustering on the first monolayer: four discrete kinetic rate equations, one for $C_{tot}$, one for $\langle x\rangle$, and one for $M_2$. These seven equations will describe any size cluster in our system.

The dimensionless cluster density distribution function, $\hat{C}_x$, is shown in Figure 1 as a function of cluster size at two different times ($\tau = 10^2$ and $\tau = 10^3$). As the clustering process proceeds in time, single atoms aggregate with each other and with larger clusters, promoting a decrease in the single-atom population and an increase in the number of larger clusters (Figure 1). Notice that the density of two-atom clusters on the substrate

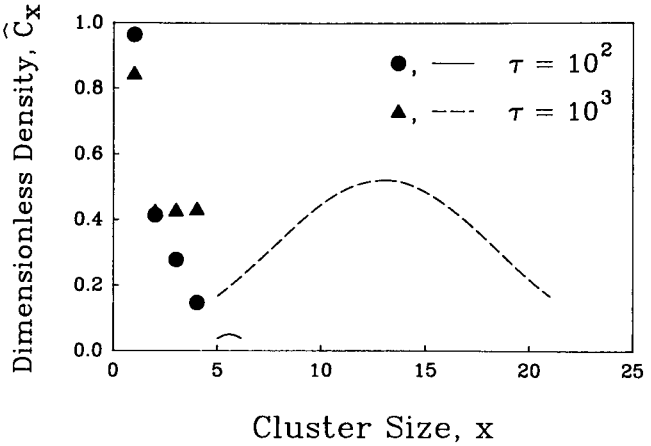


Fig. 1—Evolution of cluster distribution function at an early time ($\tau = 10^2$) and at a later time ($\tau = 10^3$). The solution of the discrete equations is represented by discrete symbols, while the solution of the continuum equation is shown by lines.

is fairly constant, while the numbers of three- and four-atom clusters rise, over the time period from $\tau = 10^2$ to $\tau = 10^3$. From the continuum curves, one sees that the total density, average size, and second moment of the continuum clusters all increase over time because of the predominance of growth mechanisms.

In Figure 1, the transition from the discrete cluster density at $x = 4$ to the continuum cluster density at $x = X_c = 5$ is marked by an apparent discontinuity in the distribution function. This mismatch is attributed to the fact that the continuum cluster distribution is assumed to be Gaussian, forcing the tail of the distribution at $x = X_c$ to an unreasonably low value. Work is now in progress to reconstruct the distribution function, including higher-order moments, which will hopefully result in a smooth transition between the discrete and continuum parts of the total distribution.

To gain more insight into the clustering kinetics, Figure 2 displays the discrete cluster densities as a function of time. Since only single atoms are being deposited, single atoms are the first entities to appear on the substrate. Each discrete cluster density is characterized by three stages: an initial growth stage, an equilibrium

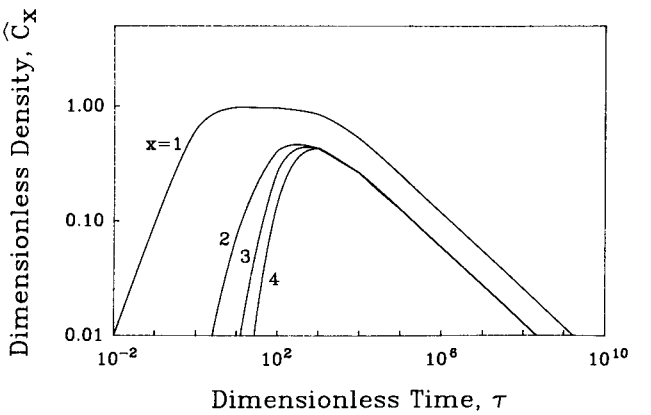


Fig. 2—Temporal behavior of single atoms ($\hat{C}_1$) and various other small-size atomic clusters.

plateau, and then a steady decline. Cluster growth is due to deposition or aggregation processes, while the cluster densities decrease as clusters aggregate to or are consumed by larger species. Each plateau represents an equilibrium between these competing growth and consumption events. Our computations show that an incubation period is required before two-, three-, and four-atom clusters are observed; this is because the production of these clusters depends on single atoms aggregating with other single atoms, and with two- and three-atom clusters, respectively. Larger clusters were not allowed to dissociate in this study (*i.e.*, $\alpha = 0$).

Figure 3 shows how the continuum cluster density varies over time. Since $X_c = 5$, all continuum curves begin with five atoms in the smallest continuum cluster. Notice that the total density of continuum clusters, the average continuum cluster size, and the second moment (*i.e.*, the area, mean, and width of the distribution) all increase as time progresses from $\tau = 10^3$ to $10^5$. This behavior is because clusters are continuously being nucleated and no cluster decay mechanisms are allowed (*i.e.*, $\alpha = 0$).

One interesting observation about the continuum cluster distribution is shown in Figure 4. Here, the ratio of the standard deviation to the average cluster size, $\sqrt{\hat{M}_2}/\langle\hat{x}\rangle$, is plotted as a function of the dimensionless time, $\tau$. For $\tau \geq 10^5$, this ratio tends to level out at a constant value of around 0.5. This implies that the distribution function at these later $\tau$ values assumes an equilibrium self-similar shape.

In order to benchmark our calculations, we compare our results to Zinsmeister's study.[17] In his analysis, Zinsmeister solved a series of discrete kinetic rate equations, whereas we model atomic clustering with a hybrid method that couples a set of discrete kinetic equations to an FP-type continuum. Figure 5 displays comparisons of single-stom density calculations, whereas Figure 6 compares aggregate cluster densities. The aggregate cluster density is defined as the total density of all clusters on the substrate minus the single-atom population. As seen in these figures, Zinsmeister's theory displays results over three regions of time. Our agreement with Zinsmeister's work is remarkable, indicating the validity of our approach.

As a measure of the numerical accuracy of our results,

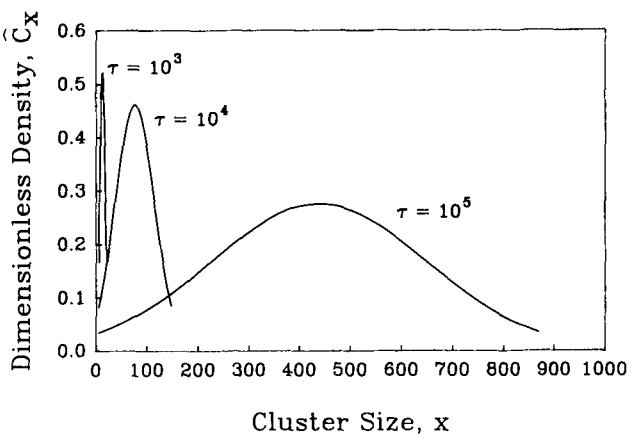


Fig. 3—Evolution of cluster distribution function resulting from solution of the continuum FP equation at various times.

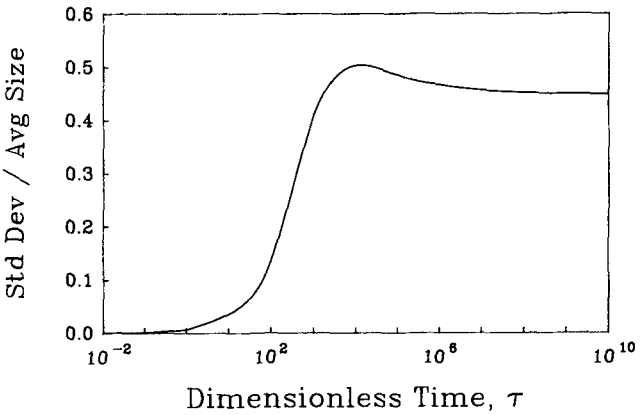


Fig. 4—Time dependence of the ratio of the standard deviation to the average size of the continuum cluster distribution function.

dimensionless atom conservation parameters are plotted in Figure 7. An atom conservation parameter (ACP) simply indicates a balance between the net number of atoms deposited on the substrate and the net number of atoms condensed in all atomic clusters. The ACP depends on both time, $t$, and where the continuum is chosen to begin in cluster-size space, $X_c$. The integral ACP is defined as

$$\text{Integral ACP}(X_c, t) = \frac{\sum_{x\geq 1}^{X_c-1} xC(x,t) + \langle x\rangle(t)C_{\text{tot}}(t)}{\int_0^t \left[q - \frac{C(1,t')}{\tau_{\text{evap1}}}\right]dt'} \quad [15]$$

and the differential ACP as

$$\text{Differential ACP}(X_c, t) = \frac{\frac{\partial}{\partial t}\left[\sum_{x\geq 1}^{X_c-1} xC(x,t) + \langle x\rangle(t)C_{\text{tot}}(t)\right]}{\left[q - \frac{C(1,t)}{\tau_{\text{evap1}}}\right]} \quad [16]$$

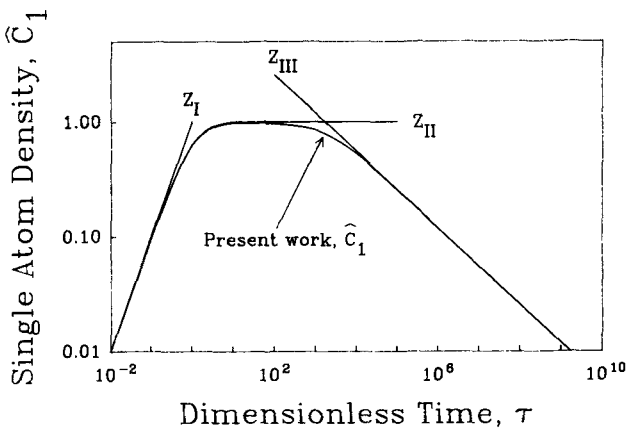


Fig. 5—A comparison between our dimensionless single-atom density ($\hat{C}_1$) and Zinsmeister's three-region theory (indicated by $Z_I$, $Z_{II}$, and $Z_{III}$).

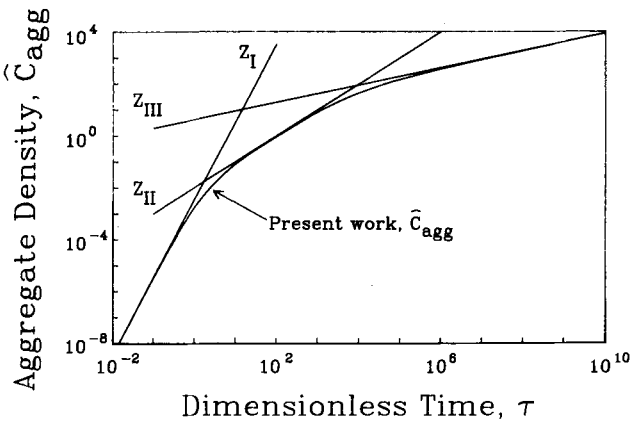


Fig. 6—A comparison between our dimensionless aggregate cluster density ($\hat{C}_{agg}$) and Zinsmeister's three-region theory (indicated by $Z_I$, $Z_{II}$, and $Z_{III}$).

Atom conservation is achieved when either of the ACPs equals 1.0. The dimensionless forms of Eqs. [15] and [16] are found in Appendix C. The results in Figure 7 indicate that a maximum error of less than 1.5 pct is achieved over 12 orders of magnitude of evolution time. This is a resonable deviation in the ACP, considering the high degree of stiffness the system of clustering equations exhibits over this period of time.

## V. DISCUSSION

The early stages of thin film formation have been described with a simple hybrid model that couples a set of discrete kinetic rate equations to an FP-type continuum. As a result, only a few equations are needed to model simple atomic clustering, the total number not being dictated by the largest cluster. For the thermal deposition process studied, the model agreement with Zinsmeister's three-region theory is remarkable under conditions where cluster dissociation is inhibited. This demonstrates that the kinetic coupling between the discrete equations and the continuum is successful.

From a numerical standpoint, the atom conservation parameters indicate that our computations are less than 1.5 pct in error. However, since the solution of our equations requires specificity as to where the continuum begins in cluster-size space (*i.e.*, the value of $X_c$), one may wonder how the calculations depend on $X_c$. For the thermal deposition process modeled in Section IV, additional computations with $X_c$ = 5, 50, 100, and 500 have shown that the clustering results do not depend on the value of $X_c$ selected. Current studies indicate that $X_c$ may influence the clustering phenomena, though, if dissociation is considered. Nonetheless, we feel confident in both the simplicity and accuracy of our model.

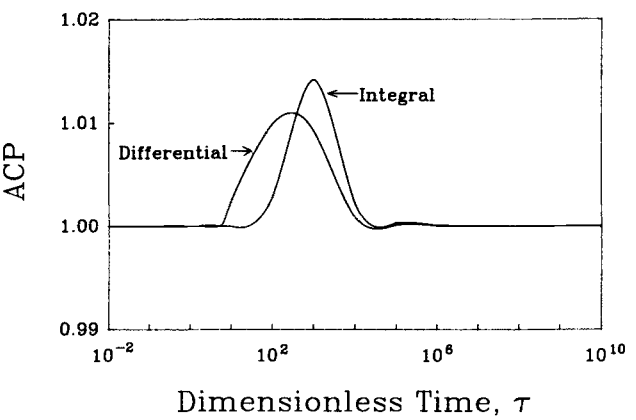


Fig. 7—Illustration of the numerical accuracy for atom conservation as a function of dimensionless time. The atom conservation parameter, ACP = 1.0, gives perfect conservation.

A question often arises concerning the length of time it takes to form a monolayer of film on a substrate. The time length depends on a variety of factors (*e.g.*, deposition rate, substrate temperature, depositing species, *etc.*). Because we have lumped several deposition parameters in the dimensionless variables $\beta$ and $\gamma$ in our nondimensional analysis (Appendix B), there is no specific time that indicates when a monolayer is formed. Two deposition experiments which are totally different in terms of monolayer formation times could be described by the same set of dimensionless parameters. Hence, the monolayer formation time is not a fixed result in our model.

Because of the simplicity and accuracy of our model, a comprehensive treatment of thin film formation by energetic atoms is feasible. The first step will be to look at the later stages of thin film formation when cluster coalescence and direct impingement effects are significant. When energetic particles are deposited, the various synergistic effects of particle reflection, sputtering, implantation, and cluster resolution will have to be considered. Also, a size-dependent aggregation factor, $w_1(x)$, and cluster dissociation rate, $\alpha_1(x)$, will be used instead of constant $w$ and $\alpha$ values. Finally, a means of using a continuum cluster density which is non-Gaussian is being developed. All of these features will be helpful in analyzing multilayer films and in characterizing their structures.

## APPENDIX A

Equation [3] represents a conservation equation for the early stages of atomic clustering, when coalescence is negligible and cluster decay and growth occur by single-atom transitions. We rewrite Eq. [3] for single-atom transitions as

$$\frac{\partial C(x,t)}{\partial t} + \nabla \cdot \mathbf{J}(x,t) = S(x,t) \qquad [A1]$$

where $S(x,t)$ is a generalized net source of atomic clusters of size $x$. During the later stages of nucleation, when cluster coalescence becomes important, Eq. [A1] will take the form

$$\frac{\partial C(x,t)}{\partial t} + \nabla \cdot \mathbf{J}(x,t) = \int_2^{x-2} w_y(x-y)C(x-y,t)C(y,t)dy - \int_2^{X_{max}-x} w_y(x)C(x,t)C(y,t)dy \qquad [A2]$$

Moments of Eq. [A2] can be obtained to derive equations which replace Eqs. [10] through [12] when cluster coalescence is considered.

## APPENDIX B

Equations [5] through [14] are nondimensionalized by defining a number of dimensionless variables and then rewriting these equations in terms of the dimensionless variables. This procedure is useful in obtaining information on many equivalent physical systems for a single solution of the dimensionless clustering equations. We define the nondimensional variables as follows:

Dimensionless time, $\tau$:

$$\tau = t/\tau_{\text{evap1}} \qquad [B1]$$

Dimensionless cluster density, $\hat{C}_x$:

$$\hat{C}_x = \hat{C}(x, \tau) = C(x, t)/q\tau_{\text{evap1}} \qquad [B2]$$

Dimensionless total density of continuum clusters, $\hat{C}_{\text{tot}}$:

$$\hat{C}_{\text{tot}} = \hat{C}_{\text{tot}}(\tau) = C_{\text{tot}}(t)/q\tau_{\text{evap1}} \qquad [B3]$$

Dimensionless average size of continuum clusters, $\langle\hat{x}\rangle$:

$$\langle\hat{x}\rangle = \langle\hat{x}\rangle(\tau) = \langle x\rangle(t) \qquad [B4]$$

Dimensionless second moment of continuum clusters, $\hat{M}_2$:

$$\hat{M}_2 = \hat{M}_2(\tau) = M_2(t) \qquad [B5]$$

Dimensionless drift coefficient, $\hat{F}$:

$$\hat{F} = \hat{F}(\tau) = F(t)\tau_{\text{evap1}} \qquad [B6]$$

Dimensionless dispersion coefficient, $\hat{D}$:

$$\hat{D} = \hat{D}(\tau) = D(t)\tau_{\text{evap1}} \qquad [B7]$$

Dimensionless nucleation current going into the continuum, $\hat{J}_{X_c}$:

$$\hat{J}_{X_c} = \hat{J}(X_c, \tau) = J(X_c, t)/q \qquad [B8]$$

We also define the following dimensionless parameters:

$$\beta = wq\tau_{\text{evap1}}^2$$

= ratio of aggregation rate to evaporation rate [B9]

$$\gamma = \alpha\tau_{\text{evap1}}$$

= ratio of dissociation rate to evaporation rate [B10]

With these definitions, the following set of dimensionless clustering equations is readily obtained:

$$\frac{\partial\hat{C}_1}{\partial\tau} = 1 - \hat{C}_1 - \beta\hat{C}_1^2 + \gamma\hat{C}_2 - \hat{F}\left[\sum_{x\geq 2}^{X_c-1}\hat{C}_x\right] - \hat{F}\hat{C}_{\text{tot}} \qquad [B11]$$

$$\frac{\partial\hat{C}_2}{\partial\tau} = \frac{1}{2}\beta\hat{C}_1^2 - 2\hat{D}\hat{C}_2 + \gamma\hat{C}_3 \qquad [B12]$$

$$\frac{\partial\hat{C}_x}{\partial\tau} = \beta\hat{C}_1\hat{C}_{x-1} - 2\hat{D}\hat{C}_x + \gamma\hat{C}_{x+1} \quad \text{for } 3 \leq x \leq (X_c - 1) \qquad [B13]$$

$$\frac{\partial\hat{C}_{\text{tot}}}{\partial\tau} = \hat{J}_{X_c} \qquad [B14]$$

$$\frac{\partial\langle\hat{x}\rangle}{\partial\tau} = \frac{[(X_c - \langle\hat{x}\rangle)\hat{J}_{X_c} + \hat{D}\hat{C}_{X_c}]}{\hat{C}_{\text{tot}}} + \hat{F} \qquad [B15]$$

$$\frac{\partial\hat{M}_2}{\partial\tau} = \frac{[(X_c - \langle\hat{x}\rangle)^2 - \hat{M}_2]\hat{J}_{X_c}}{\hat{C}_{\text{tot}}} + 2\hat{D}\left[\frac{(X_c - \langle\hat{x}\rangle)\hat{C}_{X_c}}{\hat{C}_{\text{tot}}} + 1\right] \qquad [B16]$$

where we have

$$\hat{F} = \beta\hat{C}_1 - \gamma \qquad [B17]$$

$$\hat{D} = \frac{1}{2}(\beta\hat{C}_1 + \gamma) \qquad [B18]$$

$$\hat{C}_{X_c} = \frac{\hat{C}_{\text{tot}}}{\sqrt{2\pi\hat{M}_2}}\exp\left[-\frac{(X_c - \langle\hat{x}\rangle)^2}{2\hat{M}_2}\right] \qquad [B19]$$

$$\hat{J}_{X_c} = \beta\hat{C}_1\hat{C}_{X_c-1} - \gamma\hat{C}_{X_c} \qquad [B20]$$

## APPENDIX C

Equations [15] and [16] were nondimensionalized and solved on a computer in order to obtain the atom conservation parameters depicted in Figure 7. Using the dimensionless variables defined in Appendix B, the dimensionless integral ACP is given by

$$\text{Dimensionless Integral ACP}(X_c, \tau) = \frac{\sum_{x\geq 1}^{X_c-1} x\hat{C}_x + \langle\hat{x}\rangle\hat{C}_{\text{tot}}}{\int_0^{\tau}(1 - \hat{C}_1)d\tau'} \qquad [C1]$$

and the dimensionless differential ACP as

$$\text{Dimensionless Differential ACP}(X_c, \tau) = \frac{\frac{\partial}{\partial\tau}\left[\sum_{x\geq 1}^{X_c-1} x\hat{C}_x + \langle\hat{x}\rangle\hat{C}_{\text{tot}}\right]}{1 - \hat{C}_1} \qquad [C2]$$


## ACKNOWLEDGMENT

This work was performed under appointment to the Magnetic Fusion Energy Technology Fellowship program administered by Oak Ridge Associated Universities for the U.S. Department of Energy.


## REFERENCES


1. K.J. Klabunde: *Thin Films from Free Atoms and Particles*, Academic Press, Inc., Orlando, FL, 1985, pp. 203-55.
2. O. Auciello and R. Kelly: *Ion Bombardment Modification of Surfaces: Fundamentals and Applications*, Elsevier, Amsterdam, 1984, pp. 127-62.
3. T. Sugano: *Applications of Plasma Processes to VLSI Technology*, John Wiley and Sons, Inc., New York, NY, 1985, pp. 1-3.

4. Y. Hirooka, D.M. Goebel, R.W. Conn, G.A. Campbell, W.K. Leung, K.L. Wilson, W. Bauer, R.A. Causey, D.H. Morse, and J. Bohdansky: *Nucl. Instrum. Methods*, 1986, vol. B23, pp. 458-70.
5. D.M. Goebel, Y. Hirooka, R.W. Conn, W.K. Leung, G.A. Campbell, J. Bohdansky, K.L. Wilson, W. Bauer, R.A. Causey, A.E. Pontau, A.R. Krauss, D.M. Gruen, and M.H. Mendelsohn: *J. Nucl. Mater.*, 1987, vol. 145–47, pp. 61-70.
6. Y. Hirooka, D.M. Goebel, R.W. Conn, W.K. Leung, and G.A. Campbell: *J. Nucl. Mater.*, 1986, vol. 141–43, pp. 193-97.
7. P. Sioshansi: *Thin Solid Films*, 1984, vol. 118, pp. 61-71.
8. J.W. Matthews: *Epitaxy*, Academic Press, Inc., New York, NY, 1975, pp. 381-436.
9. Panel Discussion: in *Modeling of Optical Thin Films*, M.R. Jacobson, ed., SPIE 821, Bellingham, WA, 1987, pp. 142-49.
10. D.L. Adler and B.H. Cooper: *Rev. Sci. Instrum.*, 1988, vol. 59 (1), pp. 137-45.
11. J.A. Venables: *J. Vac. Sci. Technol. B*, 1986, vol. 4 (4), pp. 870-73.
12. J.L. Katz and M.D. Donohue: *Adv. Chem. Phys.*, 1979, vol. 40, pp. 137-55.
13. J.D. Weeks and G.H. Gilmer: *Adv. Chem. Phys.*, 1979, vol. 40, pp. 157-228.
14. S.H. Bauer and D.J. Frurip: *J. Phys. Chem.*, 1977, vol. 81 (10), pp. 1015-24.
15. R. Niedermayer: *Angew. Chem. Int. Ed. Engl.*, 1975, vol. 14, pp. 212-18.
16. D.R. Frankl and J.A. Venables: *Adv. Phys.*, 1970, vol. 19, pp. 409-56.
17. G. Zinsmeister: *Thin Solid Films*, 1968, vol. 2, pp. 497-507.
18. G. Zinsmeister: *Vacuum*, 1966, vol. 16, pp. 529-35.
19. W.G. Wolfer, L.K. Mansur, and J.A. Sprague: in *Proc. Int. Conf.: Radiation Effects in Breeder Reactor Structural Materials*, M.L. Bleiberg and J.W. Bennett, eds., TMS-AIME, New York, NY, 1977, pp. 841-64.